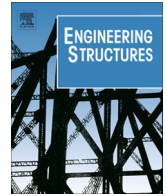




Contents lists available at ScienceDirect

Engineering Structures

journal homepage: www.elsevier.com/locate/engstruct

Impact or blast induced fire simulation of bi-directional PSC panel considering concrete confinement and spalling effect

Seung-Jai Choi, Sang-Won Lee, Jang-Ho Jay Kim *

School of Civil and Environmental Engineering, Yonsei University, 134 Shinchon-dong, Seodaemun-gu, Seoul 120-794, South Korea

ARTICLE INFO

Article history:
Available online xxxxx

Keywords:
Prestressed concrete (PSC)
Impact
Blast
Fire
Explicit FEA
Implicit FEA
RABT fire scenario

ABSTRACT

In recent years, numerous explosion and collision related tragedies due to military attack, terrorist bombing, and vehicle accident have occurred all over the world. However, researches on Prestressed Concrete (PSC) infrastructures such as Prestressed Concrete Containment Vessels (PCCVs) and LNG storage tanks under extreme loading such as impact, blast, and fire loading scenario are not being studied sufficiently. Especially, researches on possible secondary fire after bomb explosion or accidental collision on concrete structures has not been performed, while most of the past researches related to extreme loadings on structures focused on ideal isolated extreme loading event researches. Therefore, in this study, the PSC panel such as wall of PCCV and LNG storage tank is analytically evaluated under impact-blast-fire combined loading scenarios. For the analytical simulations of impact/blast and fire loaded behavior of the PSC panel, commercial finite element analysis program of LS-DYNA and MIDAS FEA, respectively, were used. Then, a simulation procedure coupling LS-DYNA and MIDAS FEA using element elimination algorithm is proposed to couple explicit and implicit finite element analyses (FEA) to perform structural analysis of impact or blast induced fire loading scenario. Then, the simulation results from the PSC and RC specimens applied with impact induced fire or blast induced fire loadings were compared with those of undamaged PSC and RC specimens. The results showed that PSC panel was more severely damaged from the fire due to the confining effect of prestressing forces. Confining effect increased the thermal conductivity of concrete due to compaction of concrete. Also, the spalling of concrete caused by impact loading followed by fire loading were implemented to the simulation model using the element elimination procedure proposed in the study. The simulation results obtained from the proposed simulation procedure agree well with the impact induced fire test results.

© 2016 Published by Elsevier Ltd.

1. Introduction

Collision accident or terrorist attack leads to detrimental explosion and catastrophic fire of structures and infrastructures. Especially, a single event of extreme load accident causes great human casualties and property damages. Furthermore, since constructions of larger, higher, more complex, and more specialized structures are becoming normal practices all over the world, the risks resulting from severe impact and fire accidents are increasing continuously. The higher risk of explosion or impact induced fire accidents occurring in densely populated cities have led to social anxiety and public concerns about catastrophic collapse of structures and infrastructures. Having recognized the need for disaster prevention system for structures against extreme loading scenar-

ios, the quantitative study to evaluate the risk of impact, explosion, and fire scenarios as well as to develop disaster control techniques have been attempted recently [1–6]. However, these studies are limited to experimental and analytical researches on concrete structure exposed to a single extreme event from an independent impact, explosion, or fire [7–10].

Literature review showed that extreme loading researches on structural member were exclusively performed for military and defense industry usages by national defense researchers or engineers where the study results are not open to public for national security reasons [11–15]. However, recently, several researchers attempted to evaluate the failure behavior of structural members exposed to real accident scenario according to actual extreme load application process [16–18].

Due to the necessity of mass generating and obtaining electricity from nuclear power reactors, the importance of securing the safety of nuclear power plants are receiving keen interest, especially after Chernobyl and Fukushima Nuclear Power Plant disas-

* Corresponding author.

E-mail addresses: seungjaechoi@yonsei.ac.kr (S.-J. Choi), lsw204@yonsei.ac.kr (S.-W. Lee), jjhkim@yonsei.ac.kr (J.-H.J. Kim).

ters. Prestressed Concrete Containment Vessel (PCCV) is the last safety barrier of a nuclear power plant in the event of nuclear reactor malfunction. Because radiation leakage from a nuclear power plant will lead to insurmountable human casualties and environment destructions that can last for centuries, the safety of the structure is vital requirement for the operation of nuclear power plants. For nuclear power plant structures, two types of possible accidental scenarios can occur: an internal pressure buildup explosion from nuclear reactor malfunction and an external extreme load application from bomb blast or airplane impact. In the past, numerous researches on the safety evaluations of internally pressurized PCCV have been conducted, but only a limited number of studies were performed on performance evaluation of external blast or impact loaded PCCVs. The reason for the lack of studies on the topic is due to the difficulties involved in obtaining precise measurements on the PSC structure under blast or impact loading. Therefore, most of the researches were performed analytically. However, the analytical results without experimental data verification are not reliable and unusable for more detailed studies. Therefore, an efficient and reliable analysis method calibrated by the experimental data on impact and fire loaded PSC structural member is urgently needed to insure the safety of nuclear power plants. In this study, a finite element simulation procedure is proposed to analyze the failure behavior of PCCV under extreme load scenario of blast or impact load induced fire. More specifically, analytic evaluations are conducted on bi-directional PSC panel member under impact induced fire load scenario to investigate its structural failure and damage pattern. Impact load was modeled as a 14 kN impactor dropped from a selected drop height and fire load was modeled as RABT fire curve. The experimental data of blast loaded reinforced concrete (RC) and impact loaded PSC panels were compared to the simulation results to verify stress and strain variations of the structure from complex behavior of confining stress and relaxation of unbonded prestressing force. Also, the experimental data for fire loaded PSC panels were compared to the simulation results to verify the thermal failure behavior. For the simulation of impact or blast loaded structures, a commercial explicit finite element program LS-DYNA was used. For the simulation of fire loaded structures, a commercial implicit finite element program MIDAS FEA was used. In order to combine the two simulation programs to conduct impact-blast induced fire loaded structural simulation, element elimination technique is used to delete elements in the structural member model that exceeded the failure state in impact or blast loading before the model is used to conduct fire simulation.

2. Experiment overview

2.1. PSC impact test

The impact experiment was conducted at the Defense Systems Test Center in the Agency for Defense Development in Korea by Yi et al. [13]. To evaluate the impact resistance performance of bi-directional unbonded prestressed concrete panel, the $1400 \times 1000 \times 300$ mm specimen was prepared as shown in Fig. 1 with reinforcement and PS tendon ratio of 0.024 and 0.0107, respectively, which are same as in nuclear containment building. PSC specimen was fabricated with D13 rebar with yield and ultimate strength of 300 MPa and 440 MPa, respectively. Concrete compressive and tensile strength was 44.2 MPa and 3.9 MPa, respectively. Impactor with weight of 1.4 tons dropped from height of 3.5 m was used for the impact test. To measure the impulse pressure from impact, a pressure disc load cell was installed between 1 ton basic weight and hemispheric head as shown in Fig. 2.

2.2. RC blast test

To calibrate the blast simulation model, the results from the blast test performed by Yi et al. were used [1]. To evaluate the blast resistance performance of reinforcement concrete panel, RC specimens with dimensions of $1000 \times 1000 \times 150$ mm were manufactured. Concrete compressive and tensile strength was 25.6 MPa and 2.20 MPa, respectively. D10 rebar with yield and ultimate strength of 400 MPa and 60 MPa, respectively, was used for reinforcement. The panel rebar layout was a mesh formation with 100 mm spacing in both directions, inserted at both top and bottom of the cross-section. It was found that ANFO 35 lbs with 1.5 m standoff distance was the most suitable loading for the test. For the behavior measurement of the specimens, the steel truss structure was constructed using SM-520, 7 mm-thick steel member as a support frame to uphold the specimen and to install measurement instrumentations underneath the specimen as shown in Fig. 3.

2.3. PSC fire only and impact induced fire tests

The results from the fire only and impact induced fire tests conducted by Yi et al. [12,14] were used to calibrate the fire simulation model. For comparison of fire only loaded specimen to impact induced fire loaded specimen, structural behavior of impact damaged PSC panels were also fire tested. Extreme fire load scenario appropriate to this study was RABT fire curve as shown in Fig. 4, in which fire temperature rose to 1200 °C within 5 min and maintained for an hour followed by the temperature degradation to room temperature over 120 min. Based on the temperature history of burning jet fuel, the closest temperature loading scenario was RABT fire curve. To check the heat transfer on concrete specimen, several k-type thermocouples were strategically placed at different specimen depth as shown in Fig. 5. The k-type thermocouple is the most common general purpose thermocouple and can measure temperature range of -200 °C to $+1350$ °C. Liquid Propane Gas (LPG) furnace used for the fire test is shown in Fig. 6. It provides the thermal heating to the bottom surface of the specimen placed on top of the furnace as shown in Fig. 6. The heat from the furnace is assumed to be applied uniformly throughout the heated bottom surface.

3. Impact, blast and fire analysis model

Impact and blast FEM analysis was conducted by using a commercial explicit finite element program, LS-DYNA. Fire FEM analysis was conducted by using a commercial implicit finite element program, MIDAS FEA. Specimen and load model and other test conditions used for the impact, blast, and fire simulations precisely followed those from the experiments.

3.1. Impact analysis

3.1.1. Finite element models and boundary condition

3D model of the specimen was generated using Hypermesh 11.0 for impact analysis. 3D solid and beam was used to model concrete and steel rebar/PS tendon, respectively. When performing numerical simulation of a concrete structure with severe stress gradient incurring from a high velocity impact, a proper mesh size is mandated to obtain accurate results. Therefore, in this study, a mesh size dependency on high strain rate simulation results from Nam et al. [15] was referred to select the element sizes. For PS tendon modelling, an individual beam element connecting two nodal points was used. A rigid body option was used for the impactor model, because impact deformation of the impactor was much less than that of the specimen. D13 rebar and PS tendon was used in

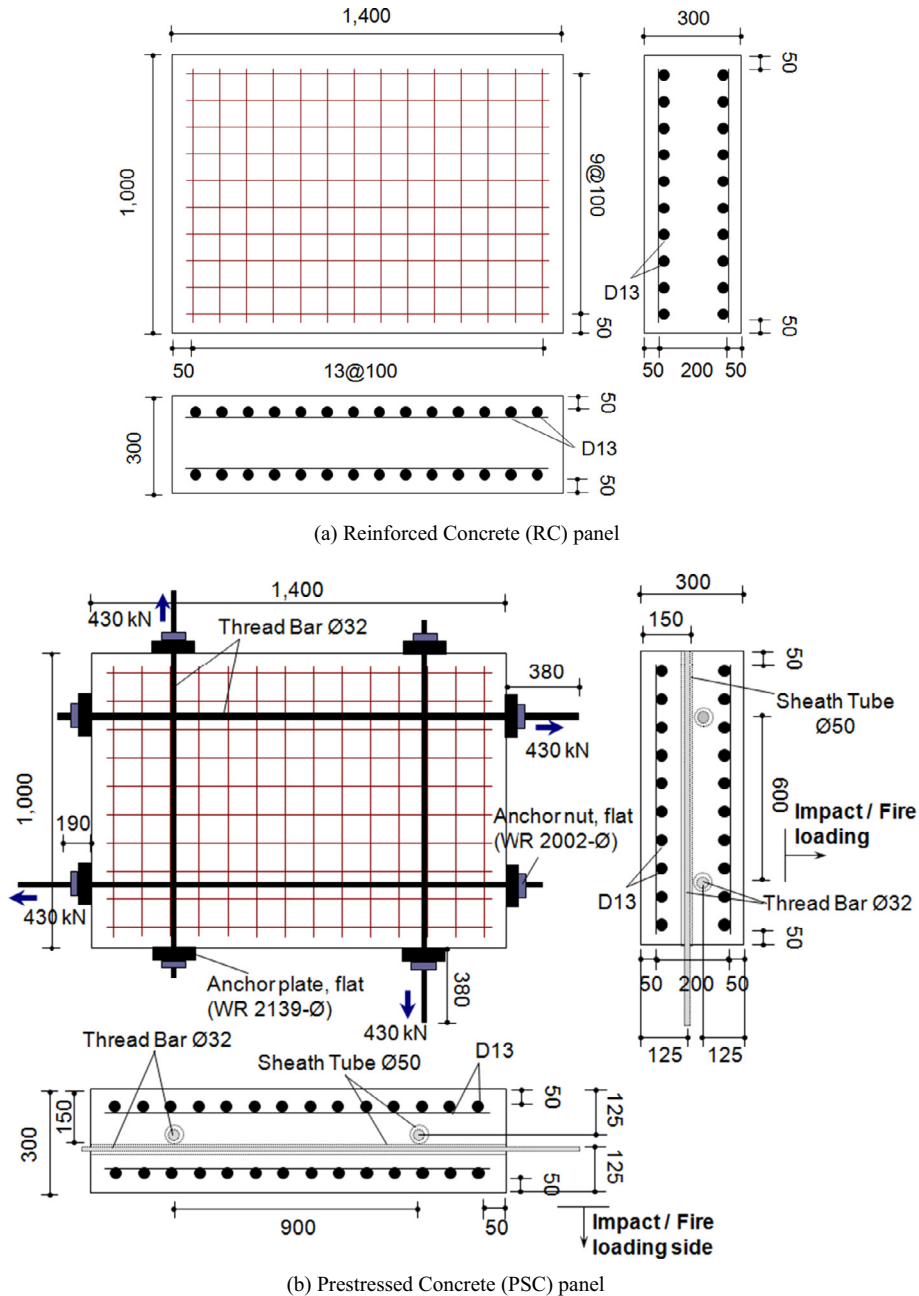


Fig. 1. Test specimen details [13].

the test was modeled as a discrete beam embedded in 3D solid concrete elements. The layout and dimensions of rebars and PS tendons followed those of the experiment precisely. Fig. 7a and b shows the FE model of RC and PSC specimen, respectively.

The steel frame and the specimen were assumed to be perfectly fixed so the steel frame and edge cover was excluded. Therefore, the top and bottom edge nodes were given fixed boundary condition. Prestressing force was implemented as initial condition for impact simulation using LS-DYNA software's Initial Stress Beam option. The initial force applied to PS tendon was assumed to be maintained throughout the simulation without any loss. The boundary between PSC specimen and impactor was implemented using LS-DYNA's Contact Algorithm (Contact Automatic One Way Surface to Surface command) based on material model incorporating constraint effect.

3.1.2. Material model

LS-DYNA offers many material cards to be used as its constitutive models, including concrete material models such as *MAT_BRITTLE_DAMAGE (MAT_96), *MAT_JOHNSON_HOLMQUIST_CONCRETE (MAT_111), *MAT_PSEUDO_TENSOR (MAT_16), *MAT_CONCRETE_DAMAGE_REL3 (MAT_72) and *MAT_CSCM_CONCRETE (MAT_159). In this study, *MAT_CONCRETE_DAMAGE_REL3 (MAT_72) and *MAT_CSCM_CONCRETE (MAT_159) were used for concrete in blast analysis and impact analysis, respectively. The description of MAT_72 and MAT_159 are clearly presented in the user's manual of LS-DYNA concrete-material Model 72 and 159, respectively [19]. The necessary parameters are derived from compressive strength measured by tests. The derived parameters are known to be suitable for concrete with compressive strength less than 50 MPa [20].

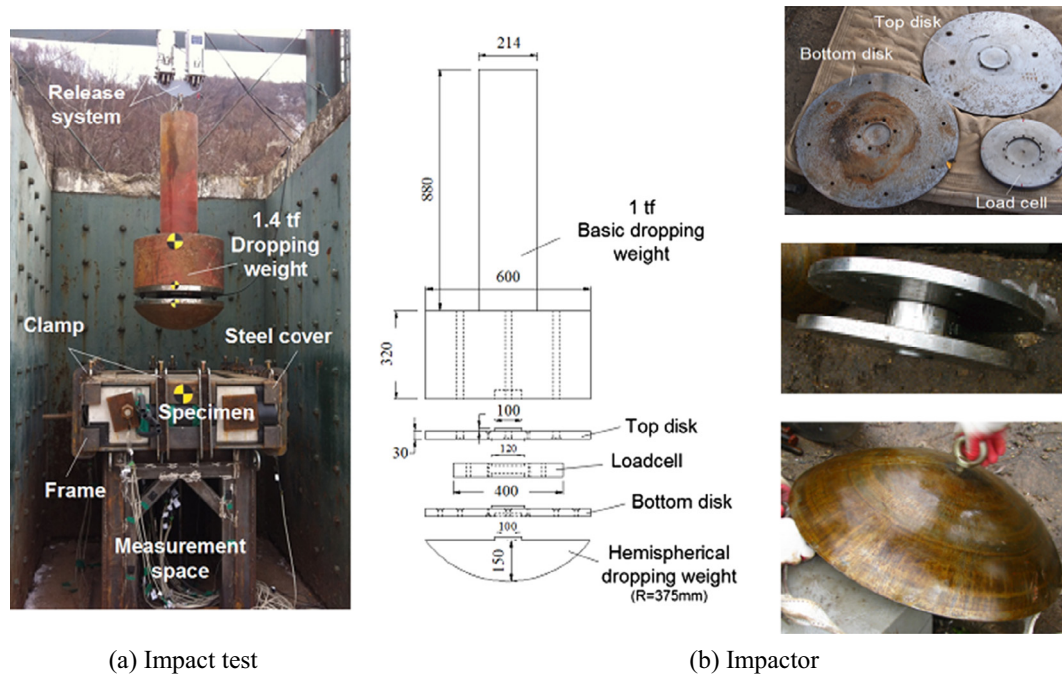


Fig. 2. Impactor details and test setup [13].

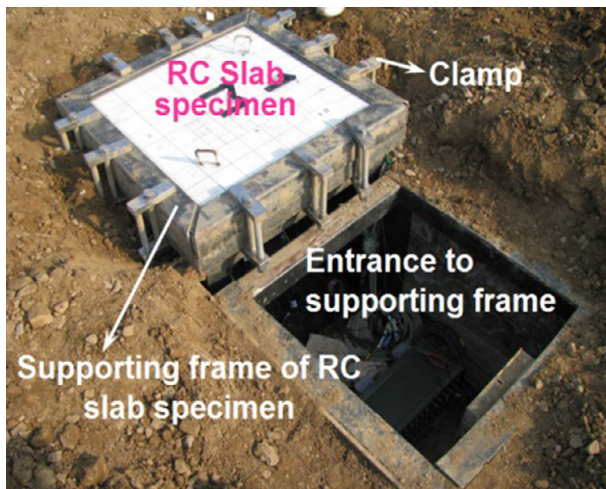


Fig. 3. Supporting frame and specimen (blast experiment) [1].

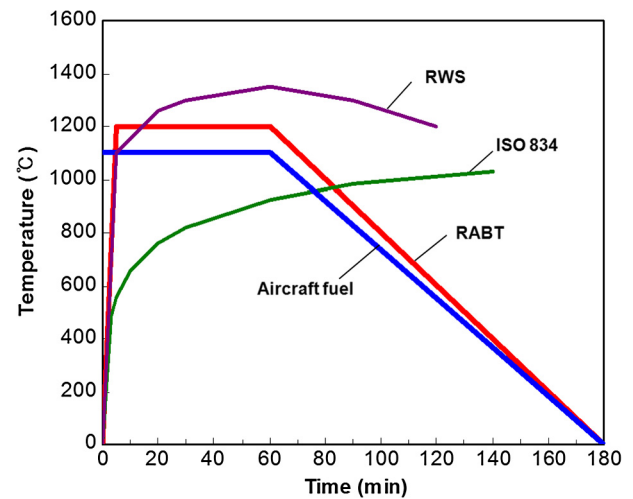


Fig. 4. Various fire temperature-time curve.

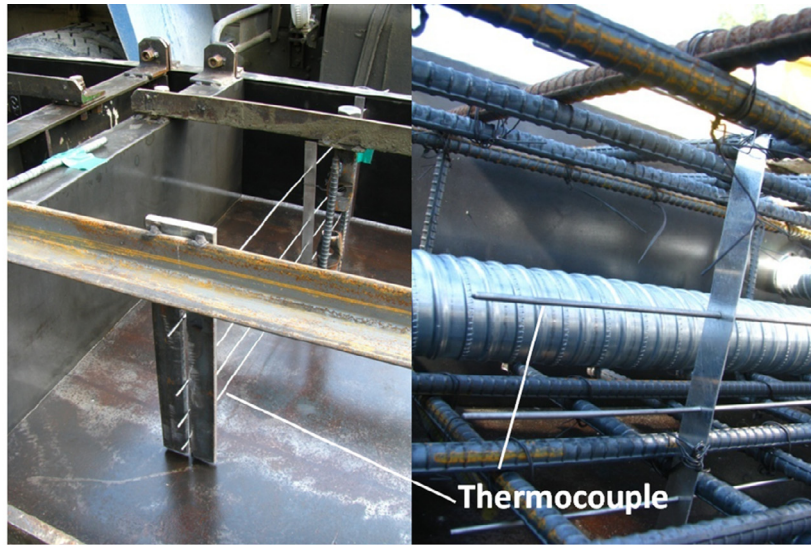
Generally, a concrete structure applied with impact load undergoes incidental nonlinear and plastic strain and damage. Therefore, the constitutive models used in the simulation must be able to reflect this high dynamic effect in the structural behavior. In this study, the concrete constitutive model developed by Malvar [21] was used in the simulation. In Malver's model, the 3 failure surfaces (elastic, plastic, residual) and tension pressure cut off are used. During initial loading or reloading, the deviatoric stresses remain elastic until the stress point reaches an initial yield surface. The deviatoric stresses can then further increase (hardening) until a maximum yield surface is reached. Beyond this stage, the response can be perfectly plastic or soften to a residual yield surface. The constitutive concrete behavior is described in Fig. 8 [22].

For rebar model, *MAT_PIECEWISE_LINEAR_PLASTICITY (MAT_24) was used. This material model takes into account isotropic and kinematic hardening plasticity. Moreover, it can define arbitrary stress versus strain curve and strain rate curve.

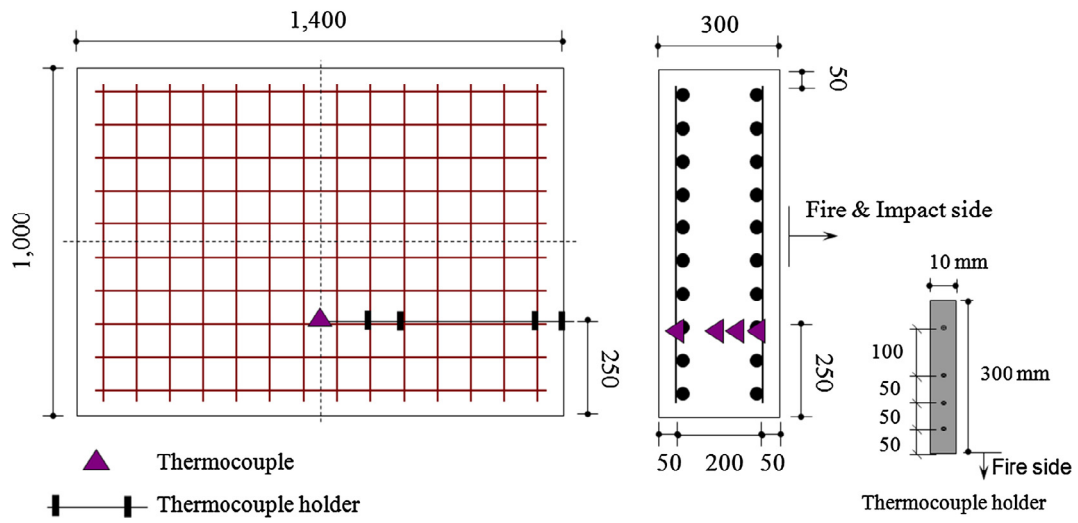
3.2. Blast analysis

For the blast simulation in this study, *MAT_CONCRETE_DAMAGE_REL3 (MAT_72), which incorporates the characteristics of blast loading was used for concrete. MAT_072R3 can incorporate the concrete strength development factor for the dynamic strain rate based on blast loading. The reliability of the material model in predicting the response of reinforced concrete structure subjected to blast loading has been demonstrated by Jiang et al. [23].

LS-DYNA provides the *LOAD_BLAST option, which simulates blast loading on a structure. In this study, the maximum pressure for reflective pressure waves from ANFO 35 lbs blast with a stand-off distance of 1.5 m from the panel was estimated. The pressures from the blast waves were applied non-homogenously to the entire top surface of the concrete panel. The time history of blast pressure and impulse are shown in Fig. 9.



(a) K-type thermocouple



(b) Thermocouple locations

Fig. 5. Installation of thermocouples [12].

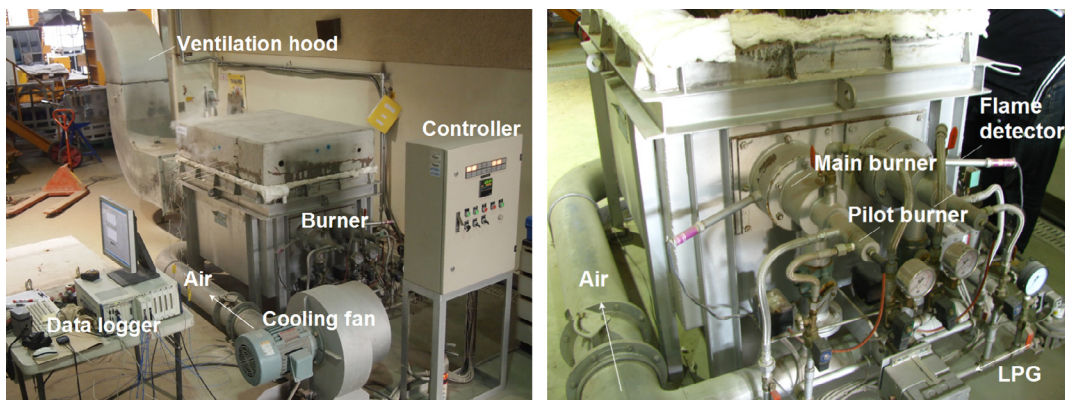


Fig. 6. Heating furnace photos [12].

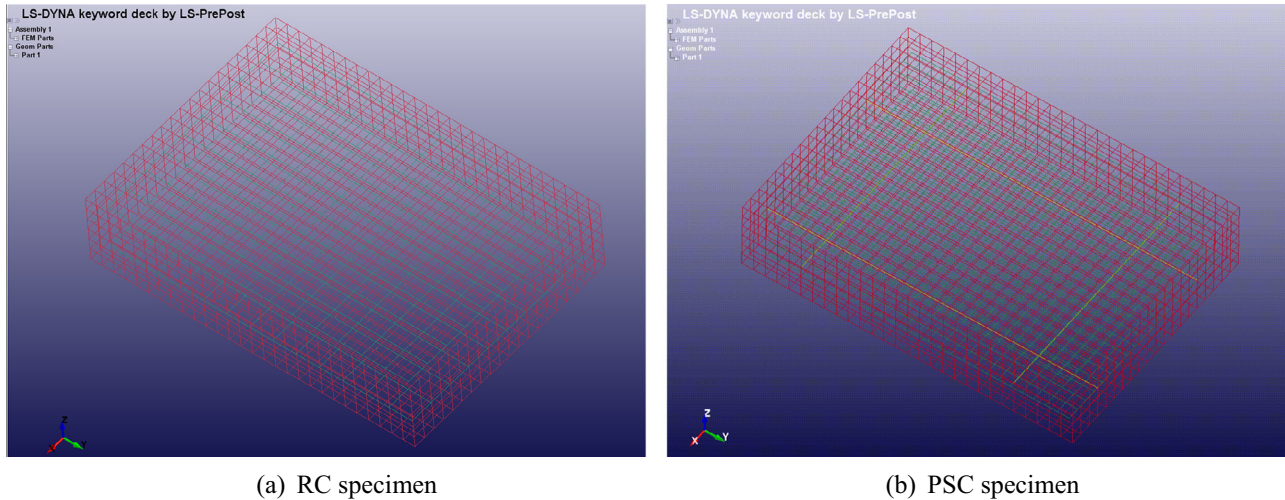


Fig. 7. Finite element model for LS-DYNA simulation.

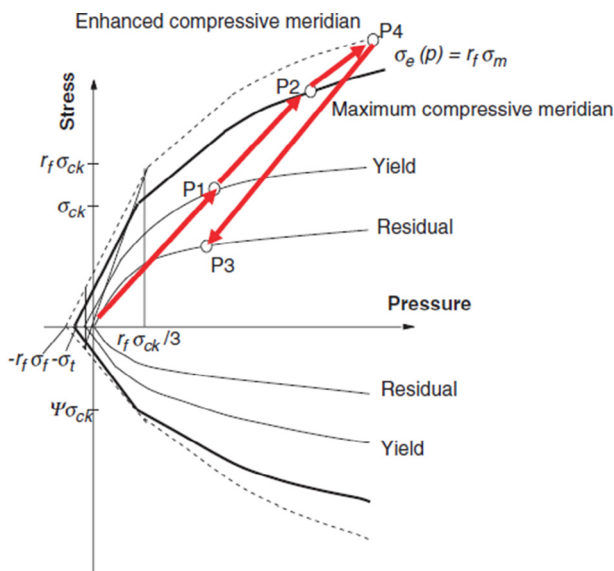


Fig. 8. Failure surfaces of concrete model [22].

3.3. Fire analysis

Variables of fire analysis were selected to precisely model the simulation conditions to the test conditions. The surface without fire load was given a boundary condition of 20 °C temperature, equivalent to a room temperature at the time of the test. Moreover, temperature dependent thermal properties of concrete such as elastic coefficient, heat expansion coefficient, and specific heat were incorporated in the simulation. As shown in Fig. 10, temperature dependent elastic coefficient and heat expansion coefficient of concrete were used. Also, as shown in Fig. 11, temperature dependent specific heat and heat conductivity of steel rebar and PS tendon were used. For example, thermal conductivity of concrete is EuroCode 2 proposes temperature dependent thermal conductivity of concrete in the range of 1.36–2.3 W/m °C [24]. However, when a general range of thermal conductivity of concrete was used in the fire simulation, the simulation results were very different to the experimentally measured temperature data. Thermal conductivity of concrete has a large variation depending on the type of aggregate, specific gravity, strength of concrete. In addition, it is very sensitive the surrounding temperature such as burning or freezing condition. Therefore, thermal conductivity must be

determined experimentally. In this study, in order to calibrate the fire simulation model to accurately represent the fire test condition, thermal conductivity of approximately five times the Euro-Code 2 proposed range (e.g., final thermal conductivity range of 5.9–12.0 W/m °C) was used in the fire simulation.

4. Impact or blast induced fire analysis procedure

To evaluate damage and failure behavior of concrete members under extreme loading, impact, blast, and fire analyses were conducted using LS-DYNA for high strain rate cases and MIDAS FEA for quasi-static rate cases. Critical state (failure or non-failure) of concrete elements after the application of extreme load was evaluated in impact and blast analyses. The concrete element was eliminated when the maximum concrete strain of 0.003 is exceeded. The critical strain value used in the study was referred from the critical compressive strain value suggested by ACI 318 as 0.003. Even though the critical strain value would probably be higher due to the high strain rate effect of impact loading, the study used a regular static strain limit value to be conservative in calculating the results. Concrete element numbers that need elimination can be found in the output data file. The concrete element number was extracted using MATLAB program, a technical computing language, in the output file to eliminate corresponding concrete elements in the specimen model for MIDAS FEA simulation or fire analysis. Through this element elimination process, the concrete exfoliation characteristic of RC and SPC specimens applied with impact or blast load can be implemented in the LS-DYNA analysis. Also, once the concrete exfoliated impact or blast damaged specimen model is achieved, then a more realistic fire simulation of damaged RC or PSC specimens is possible in MIDAS FEA fire simulation. In other words, if the concrete surface section spalls off and the rebar is exposed, the fire applied to these concrete surface exfoliated specimen would undergo greater thermal damage than that without the damage. As shown in Fig. 12, impact induced fire analysis of RC and PSC specimen was conducted implementing concrete surface spalling characteristic from impact or blast loading.

5. Analysis model verifications

5.1. Impact simulation model verification

5.1.1. von Mises stress and crack area rate results

The distribution of von Mises stress on a PSC specimen from a freefall load of a 14.2 ton impactor dropped from 3.5 m height is

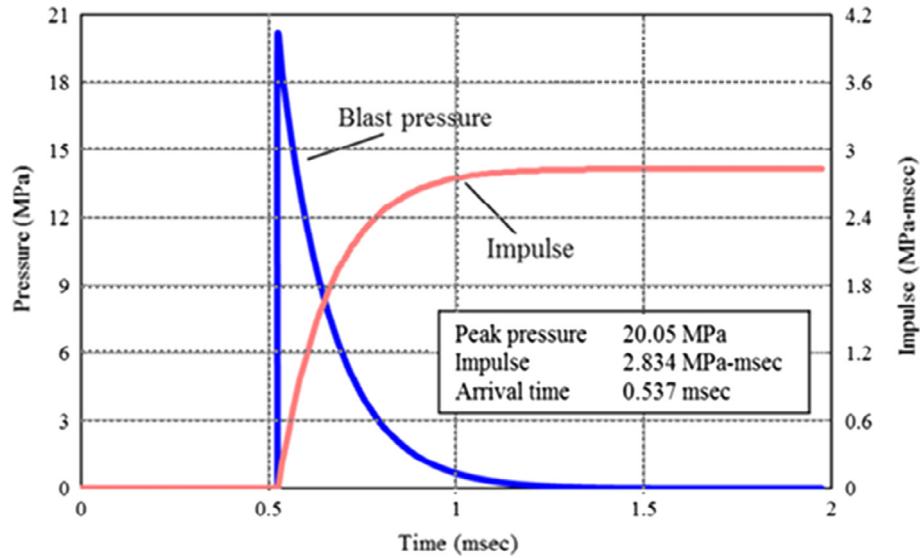


Fig. 9. Pressure-time history ANFO 35 lbs for blast analysis [1].

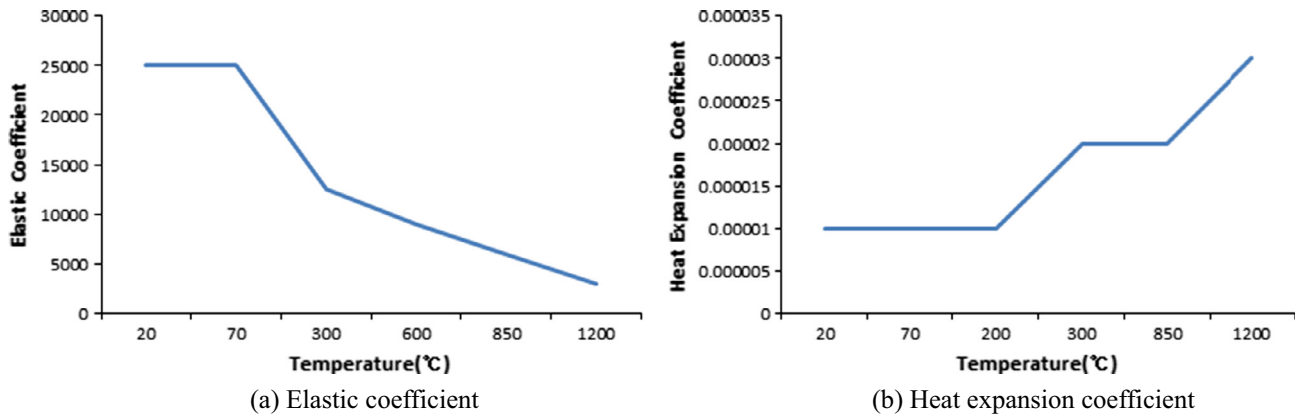


Fig. 10. Temperature dependent properties of concrete.

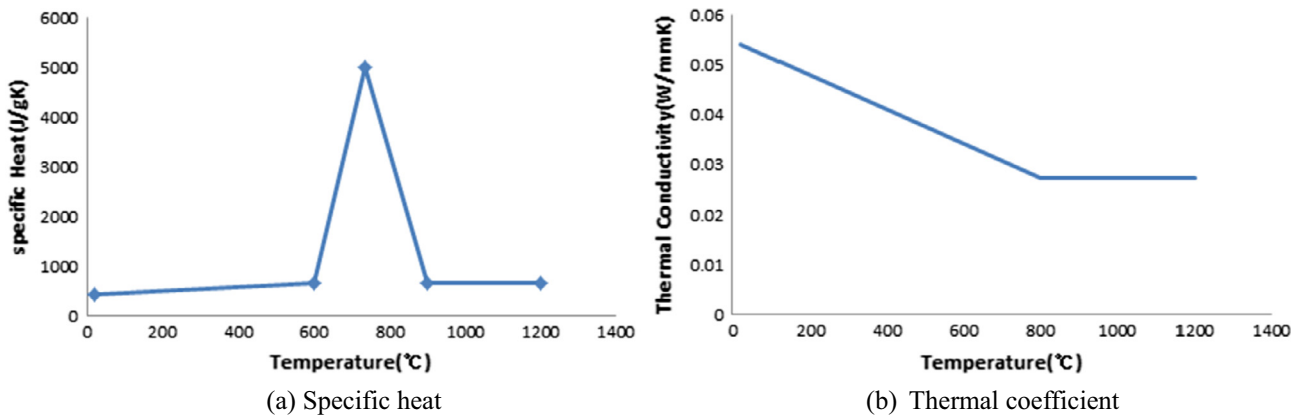
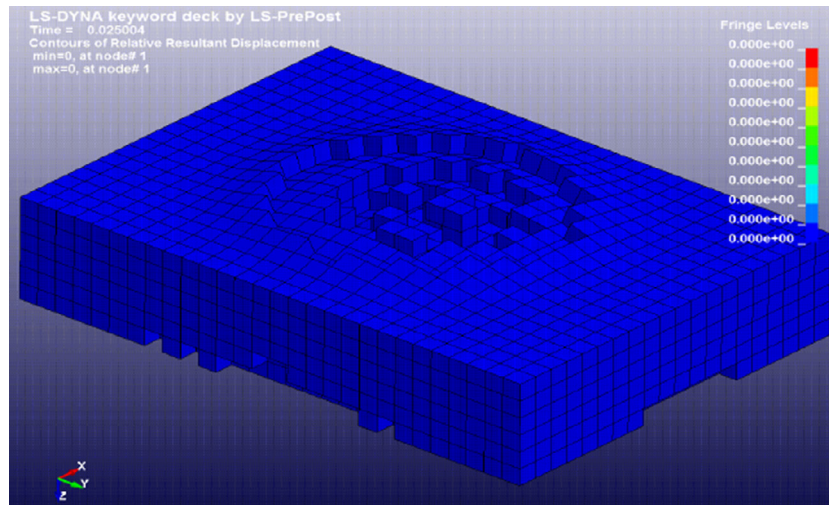


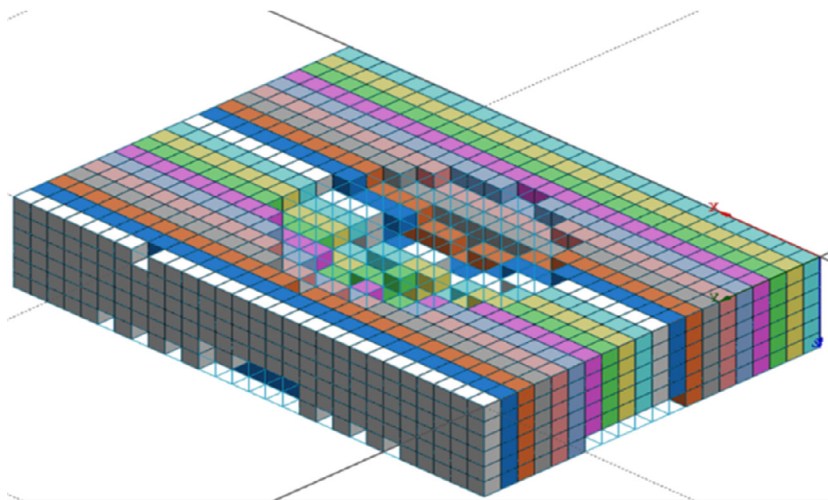
Fig. 11. Temperature dependent properties of steel rebar and PS tendon.

shown in Fig. 13. The figure shows that the specimen is applied with a great magnitude of impact load due to its instantaneous impact characteristic. Also, the stresses from the impact are transferred from top surface to the bottom, causing the concrete exfoliation at the bottom surface. For PSC specimens, the distribution of bottom surface stress is lower than that of RC specimen. Impact

simulation results of the concrete exfoliation of the specimens from the eliminations of the concrete elements are shown in Fig. 14. In the analysis results, it is unable to identify small crack due to a problem with element size, but spalling area, penetration depths, exfoliation volume are well represented. It was confirmed that 347 and 247 elements for RC and PSC specimen, respectively,



(a) Concrete exfoliation from impact simulation



(b) Specimen model of impact induced fire simulation

Fig. 12. Impact induced fire simulation.

eliminated due to exfoliation. Crack area rate is calculated by dividing the total crack area by surface area. The crack area rate comparison between the impact test and simulation results for RC and PSC specimen showed 16.28–16.13% and 9.4–11.6%, respectively. The similarity of the test to simulation results showed that the impact simulation model is valid and can be used to conduct further studies. The simulation results of crack area rate showed that PSC specimen has better impact resistance performance than RC specimen.

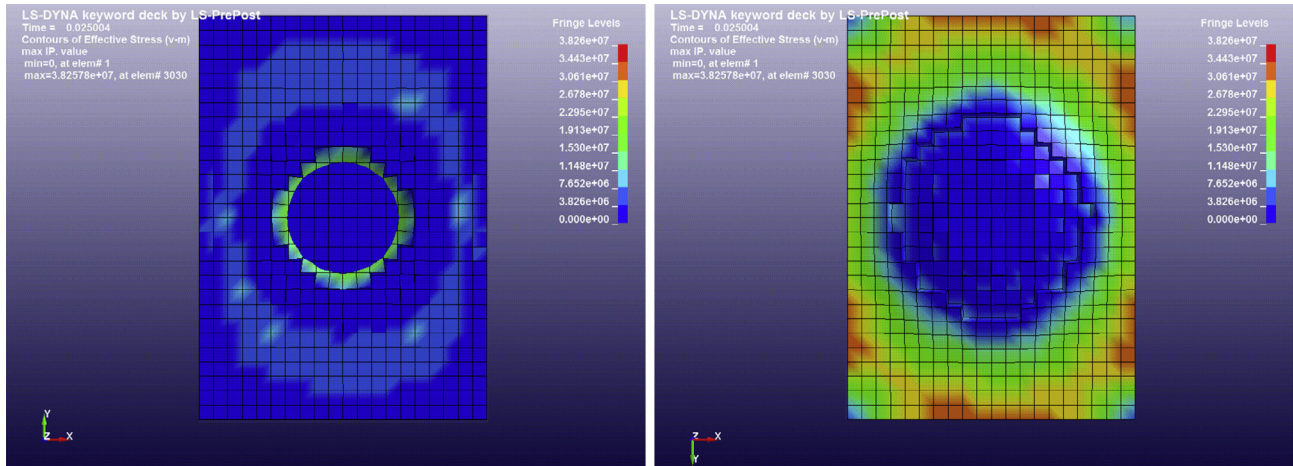
5.1.2. Impact load results

Impact load measured from RC specimen at a same location experimentally and analytically are shown in Fig. 15a and b, respectively. The maximum impact load from the experiment was 13,445 kN and 12,844 kN for RC and PSC specimen, respectively. The maximum impact load from the simulation was 12,434 kN and 12,114 kN for RC and PSC specimen, respectively. The time to reach an impact load magnitude of 10,000 kN was 0.0018 s and 0.0014 s from the test and simulation, respectively. The similarity of the test to simulation results showed that the

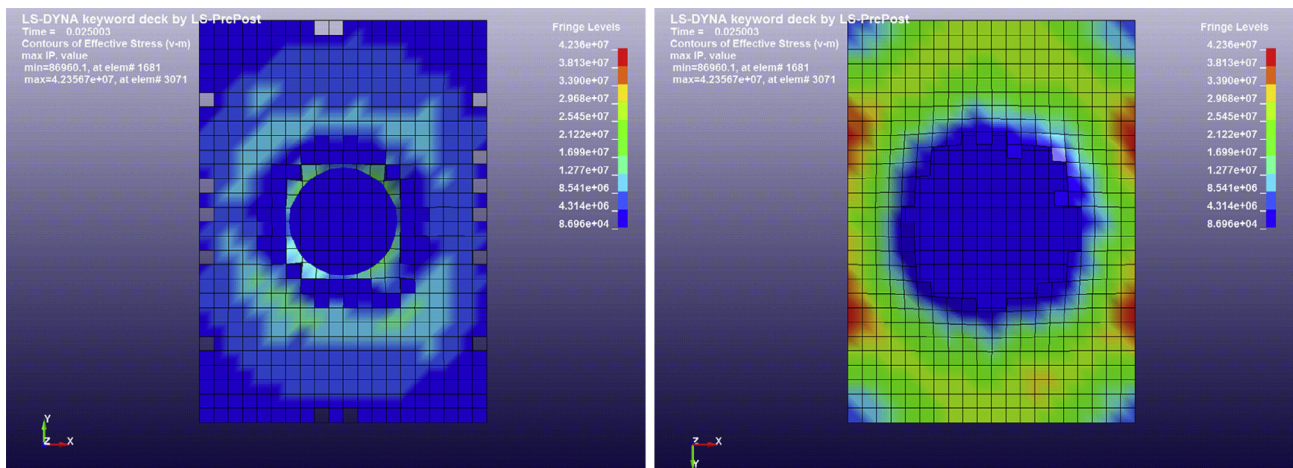
impact simulation model is valid and can be used to conduct further studies.

5.1.3. Energy results

Various energies generated from impact simulation are investigated. From the impact simulation, internal energy was regarded as absorbed energy by comparing kinematic and internal energies. It is possible to assume equivalency between the two energies, because the potential energy can be converted into kinematic energy of a dropper weight and the absorbed energy is then converted into the kinematic energy of the impacted specimen, the size of crater created by collision, crack area, exfoliation area, etc. based on the energy conservation law. Fig. 16 represents comparison of the simulation and test results of internal energy for RC and PSC specimens. The absorbed energy from the test was approximately 351.22 kJ and 344.6 kJ for RC and PSC specimen, respectively. The absorbed energy from the simulation was approximately 345.73 kJ and 322.6 kJ for RC and PSC specimen, respectively. The results from the test and simulation were very similar, except that the energy was slightly lower than the test data



(a) Top and bottom surfaces of RC specimen



(b) Top and bottom surfaces of PSC specimen

Fig. 13. Distribution of von Mises stress from impact simulation.

due to a slightly lower impact load obtained from the simulation result.

5.1.4. Displacement and acceleration results

Specimen displacement from the impact was measured at the center of panel. As shown in Fig. 17, maximum displacement at the center from the test was -21.44 mm and -50.96 mm for RC and PSC specimen, respectively. From the simulation, the maximum displacement at the center was -20.40 mm and -51.01 mm for RC and PSC specimen, respectively. The similarity of the test to simulation results once again validates the model. Displacement of PSC specimen was significantly greater than that of RC specimen, because of the existence of inherent interface between PS tendon and concrete, creating a member with lower stiffness.

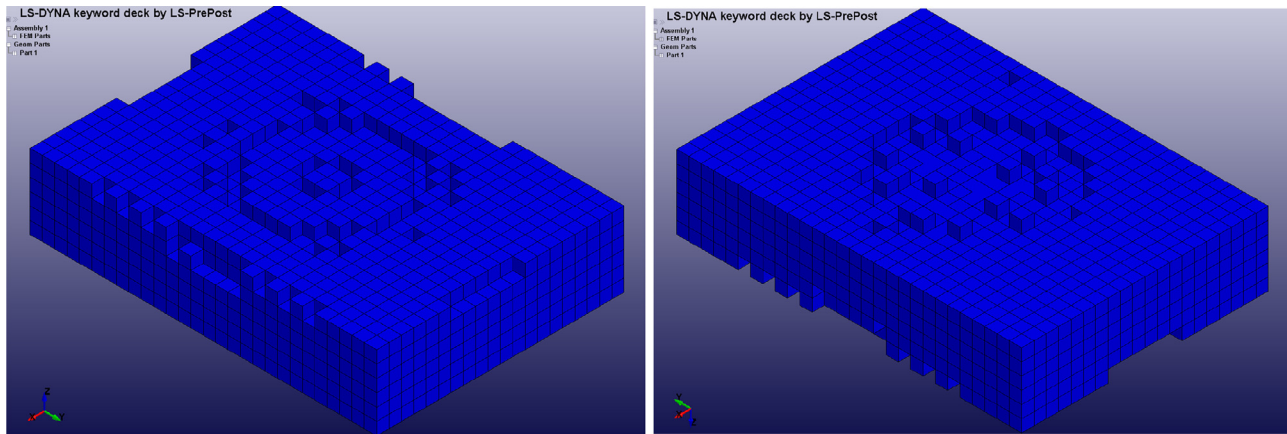
Acceleration results obtained experimentally and analytically from RC and PSC specimens are shown in Fig. 18. The maximum acceleration from the test was 1750.99 g and 1618.02 g for RC and PSC specimen, respectively. From the simulation, the maximum acceleration was 1854 g and 1637.77 g for RC and PSC specimen, respectively. Due to the acceleration effect of the specimens, the absorbed energy of PSC specimen was converted

into kinematic energy by 1.25 times greater than that of RC specimen.

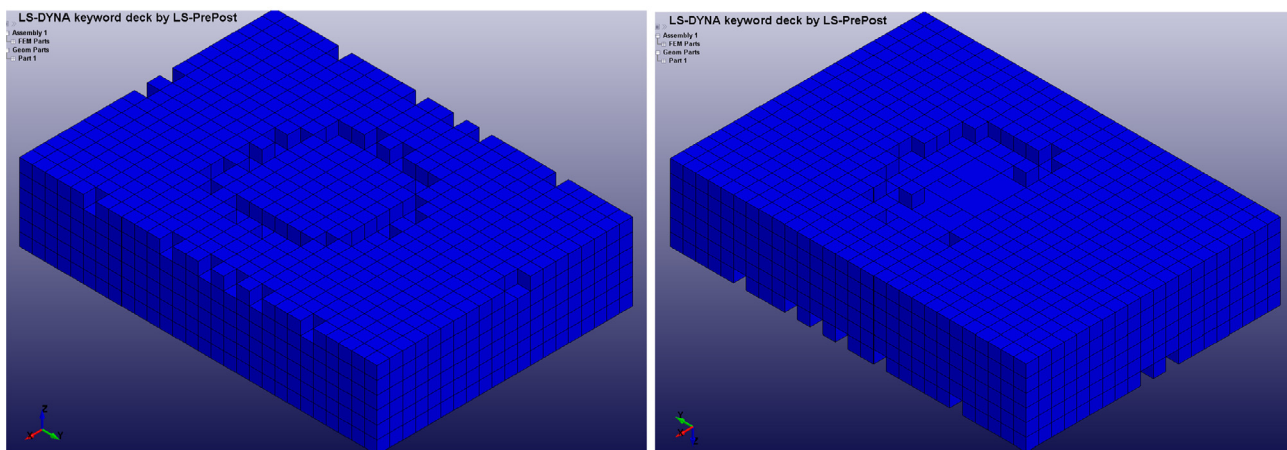
5.2. Blast simulation model verification

In the experiment, deflection behavior at the center of the specimen was measured using LVDT. As shown in Fig. 19, maximum displacement at the center was 24.40 mm and 27.01 mm from the test and simulation, respectively. The comparison between experimental and analytical results showed that the maximum deflection and residual displacement results were within the experimental margin of error.

In order to verify the accuracy of analysis results, hourglass energy must be confirmed. Hourglass energy is equivalent to artificial strain energy where a smaller value of hourglass energy indicates a more accurate simulation results. The accrued value of hourglass energy was found to be nearly less than 1.0% of the internal energy as shown in Fig. 20, which is far smaller value than the acceptable limit defined by the developers of LS-DYNA as less than 10% of the internal energy [25]. The hourglass energy evaluation of results of the blast loaded PSC panel member once again confirmed that the simulation model is accurately represents the real blast behavior of RC panels.



(a) Top and bottom surfaces of RC specimen



(b) Top and bottom surfaces PSC specimen

Fig. 14. Concrete exfoliation results from impact simulation.

5.3. Fire simulation model verification

The fire simulation is performed on the concrete panel specimen applied with thermal loading of RABT scenario at the bottom surface under the identical condition as the fire test. Temperatures at different section depth were continually obtained by placing 4 thermocouples at 5 cm, 10 cm, 15 cm, and 25 cm from heated surface. Temperature versus time relations at the thermocouple positions for RC and PSC panels are shown in Figs. 21 and 22, respectively. After 180 min into testing, temperature on PSC panel was higher than RC panel, because the PS force loss started at 60 min into testing reduced the confining stress applied to the area circumvented by the PS rods and generated more cracks to accelerate heat transfer.

Temperature versus time history curves of RC and PSC panel from the test and simulation are shown in Fig. 23. In case of RC panel, Temperature-time history curve measured at a depth of 5 cm from the test and simulation was very similar in both RC and PSC panels. The maximum temperature at a depth of 5 cm from heating surface from the test and simulation was 780 °C and 750 °C, respectively, indicating that a difference is approximately 3%. At the maximum temperature occurrence time, the slope of temperature-time history curve from the test was steeper than that from the simulation. The difference between two slopes would explain the slight difference between the experimental and analytical maximum temperature based on approximate theory of

finite element analysis. For PSC panels, the maximum temperature at 5 cm from heating surface from the test and simulation was 1180 °C and 1050 °C, respectively. The larger difference between the test and simulation in PSC panel is the fact that the PS loss is more significant in the test than the simulation. Also, PS loss induced surface concrete exfoliation was not considered in the simulation. However, the difference was still less than 10% where the simulation model can still be considered precise and accurate.

The fire damage extent comparisons of RC and PSC panels from the test and simulation are tabulated in Table 1. According to International Tunnel Association (ITA) Guidelines, the temperature criterion for concrete damage is set as 380 °C. This criterion was used to determine thermal damage depth. The extent of the damage was analyzed by maximum thermal damage depth, time to reach maximum thermal damage depth, and time to expose rebar. In general, the fire simulation results indicated that PSC specimens were more significantly damaged than RC specimens. Moreover, the test and simulation results on thermal damage pattern were substantially similar. Based on the test and simulation results of maximum thermal damage depth, bottom rebars (rebars closer to the heated surface) were exposed in RC specimens. However, in PSC specimens, both upper and bottom rebars were exposed. The significant difference in the thermal damage depth between RC and PSC specimens showed that PSC member is more vulnerable to fire than RC members. This conclusion is reasonable, because PSC member are more prone to thermal spalling than RC member due to higher stiffness

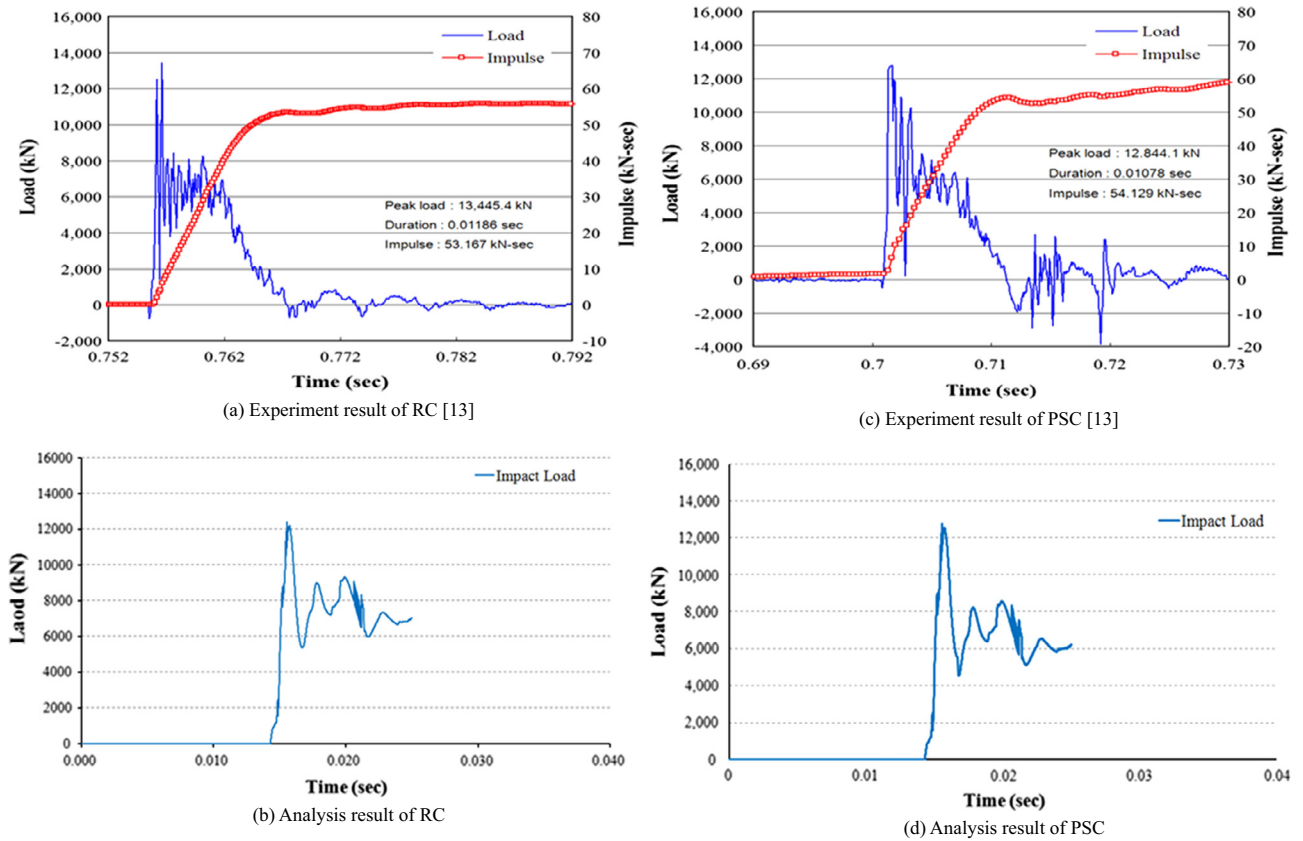


Fig. 15. Impact load results from impact test and simulation.

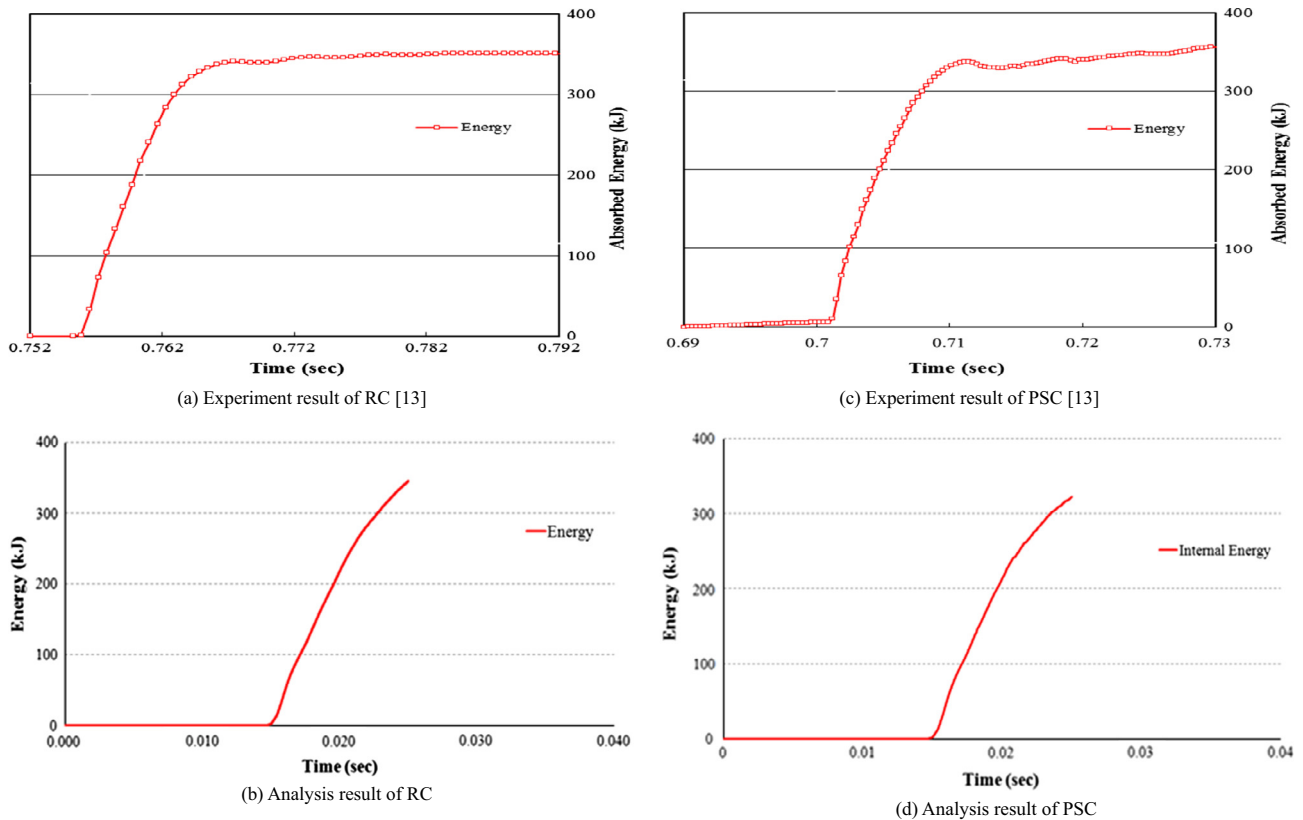


Fig. 16. Energy absorption results from impact test and simulation.

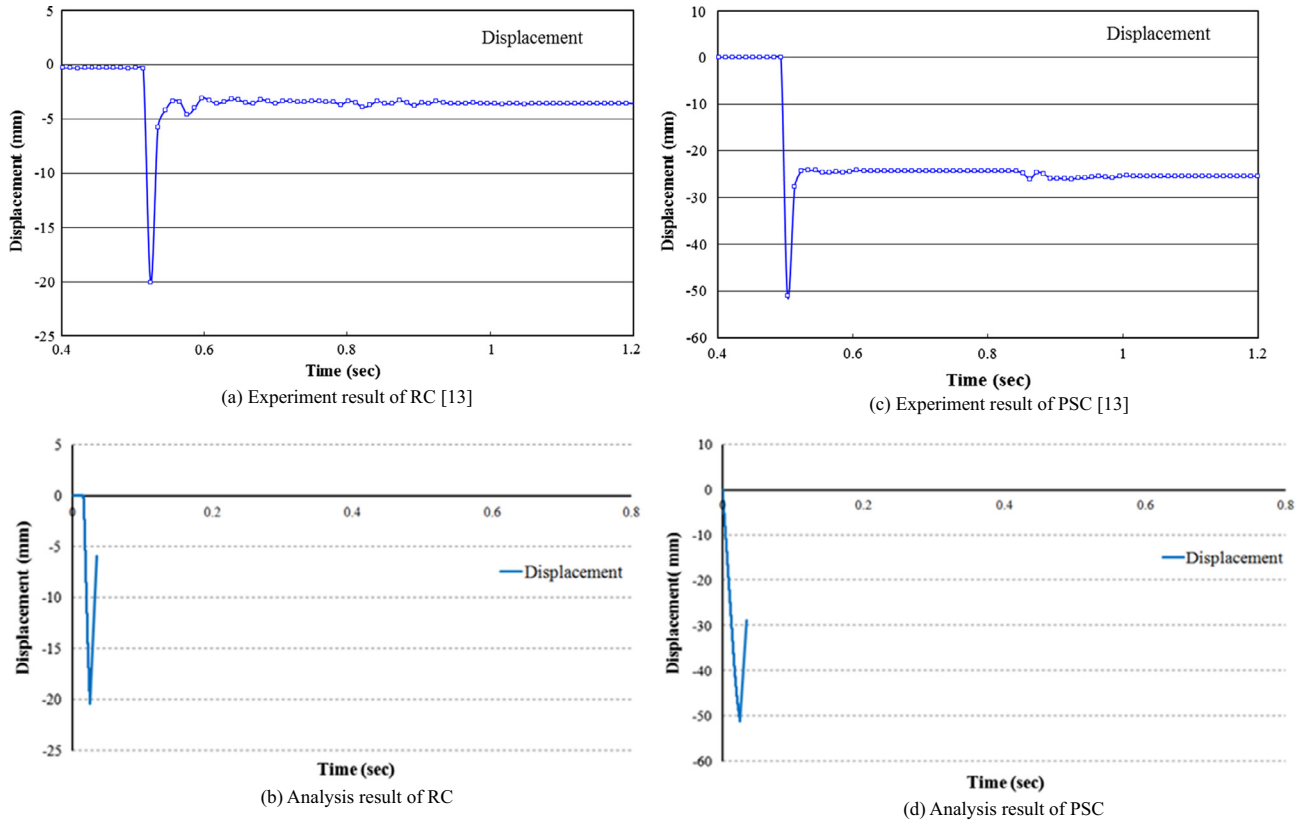


Fig. 17. Specimen displacement results from impact test and simulation.

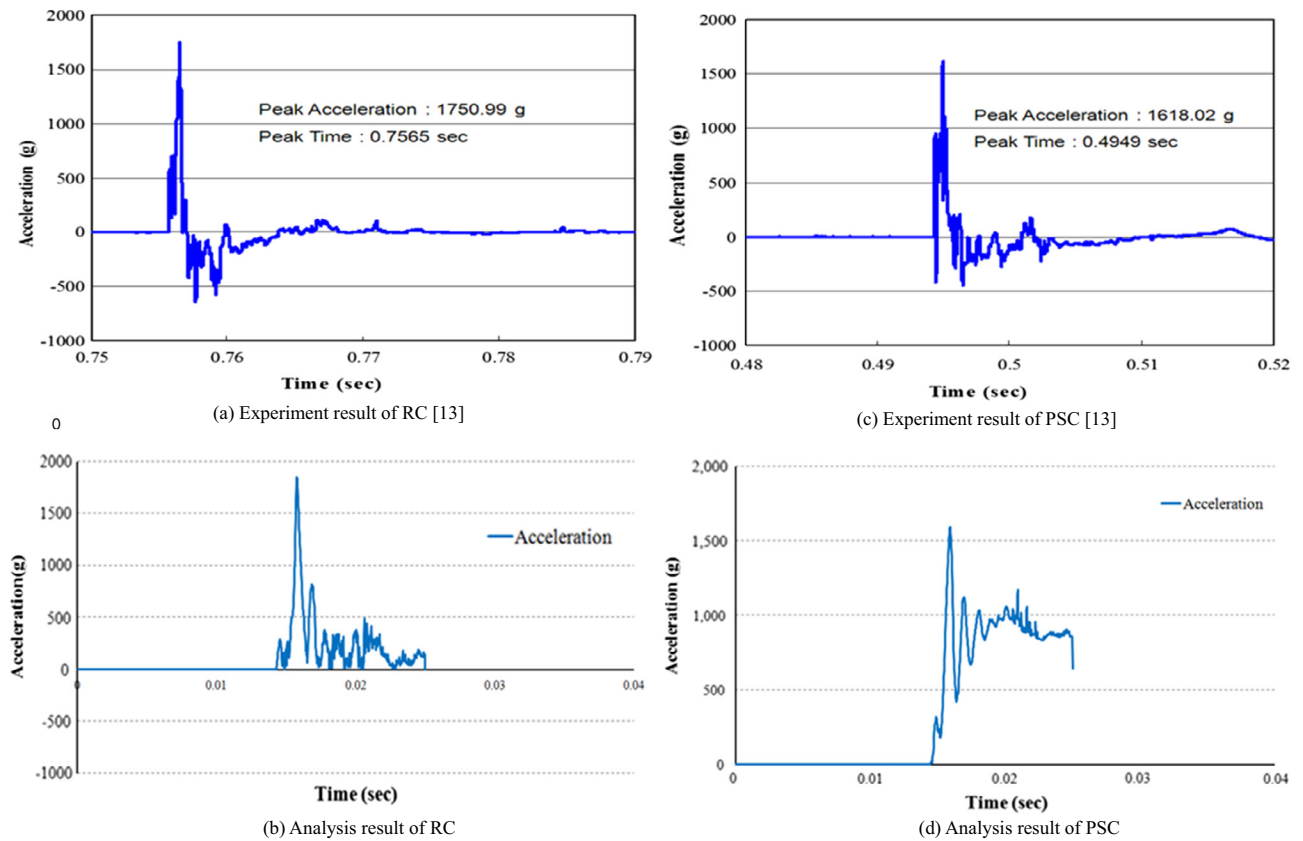


Fig. 18. Specimen acceleration results from impact test and simulation.

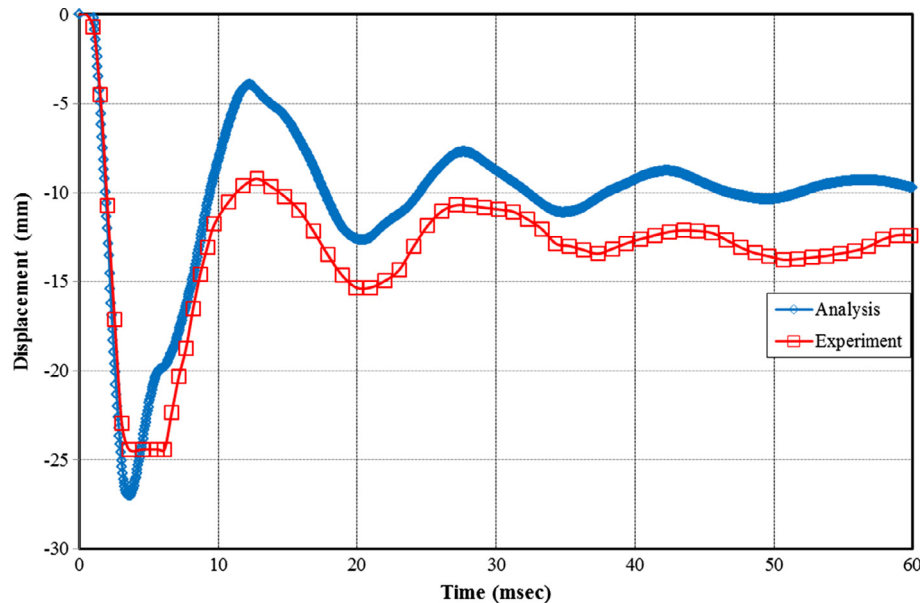


Fig. 19. Comparison of displacement results from blast test and simulation.

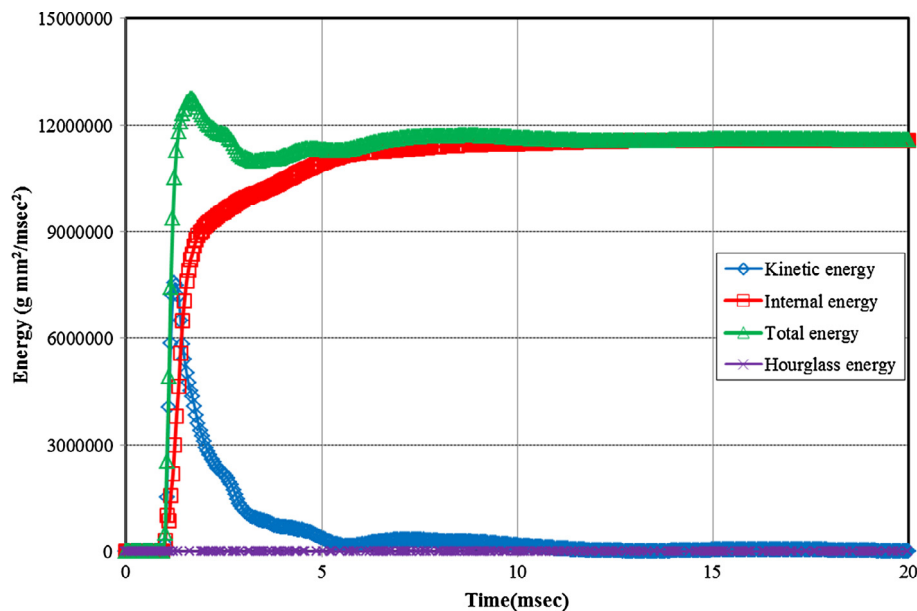


Fig. 20. Hourglass energy results from blast simulation.

of PSC member than RC member due to usage of higher strength concrete and PS force.

5.4. Impact induced fire simulation model verification

As same as in Section 5.3 “Fire simulation model verification”, the variations of elastic coefficient, heat expansion coefficient, specific heat, and heat conductivity are applied to concrete, rebar, and PS rod. More specifically, the thermal conduction on the exfoliated area would be achieved by applying heat convection of the air for the impact damaged specimen. Fig. 24 describes the top and bottom surfaces of exfoliated finite element panel models for RC and PSC specimens for the fire simulation.

The temperature distribution results for RC and PSC panels from the simulation of impact induced fire scenario are shown in Figs. 25

and 26, respectively. Fire scenario of RABT was applied on the impact caused exfoliated surface. Temperature distribution reaching the top surface (surface opposite to the fire loaded surface) at 60 min into fire loading for RC and PSC panel is shown in Figs. 24d and 25d, respectively. At 90 min into fire loading, the temperature reduction in impact induced fire specimens were more significant than fire only specimen, showing the thermal release effect from the elimination of concrete elements. The comparison of the temperature variations of impact induced fire test and simulation results are shown in Fig. 27. Remarkably, the test and simulation curves are extremely similar. This range of accuracy can only be achieved through the elimination of impact damaged concrete elements prior to performing fire simulation. Especially, the modelling of thermal heat loss through cracks in impact induced exfoliated specimen was achieved accurately by the quick

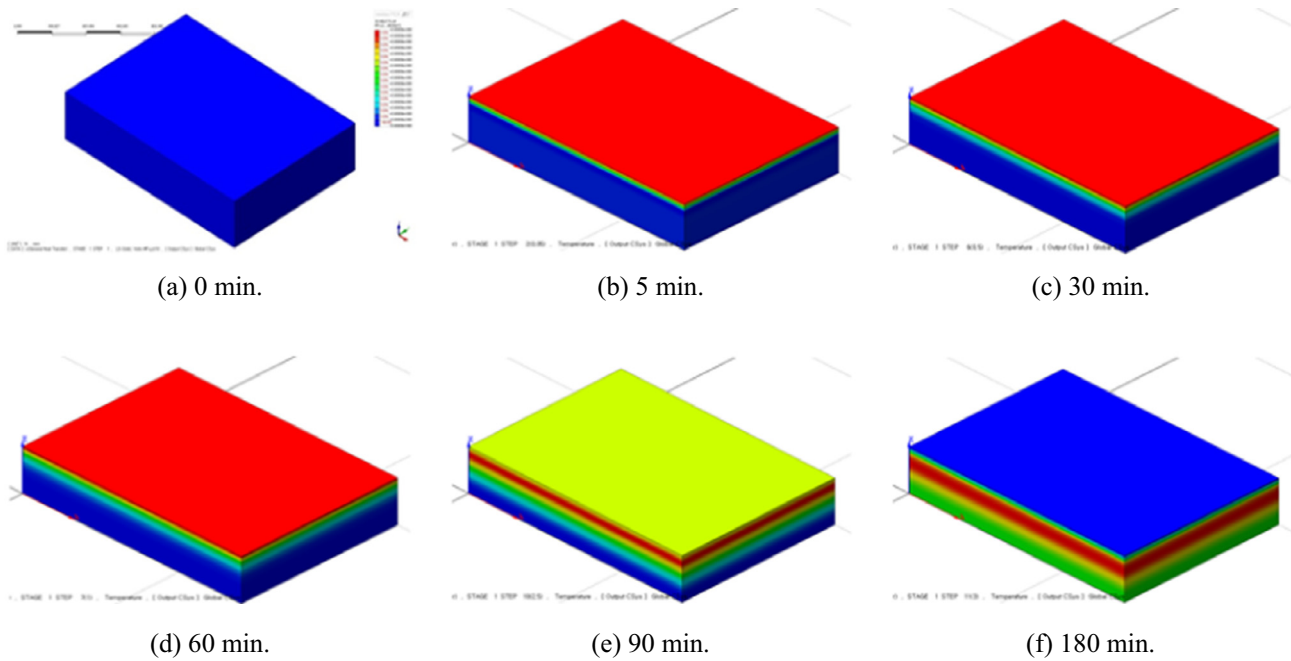


Fig. 21. Temperature distribution of RC specimen from fire only simulation.

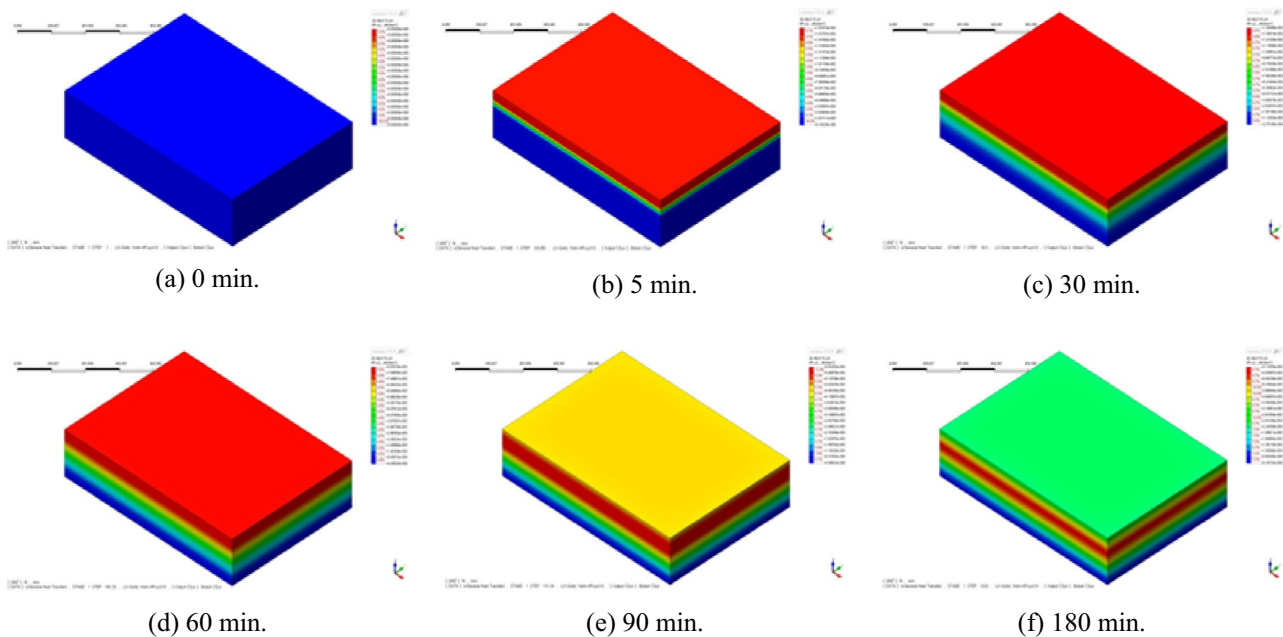


Fig. 22. Temperature distribution of PSC specimen from fire only simulation.

heat discharge effect due to eliminated concrete elements from impact exfoliation. For both RC and PSC panels, temperature-time history curves from the test and simulation panels were similar at 5 cm depth from heating surface. The maximum temperature at 5 cm depth from heating surface for RC specimen from the test and simulation was 860 °C and 840 °C, respectively, which is a difference of less than 2.5%. The maximum temperature at 5 cm from heating surface for PSC specimen from the test and simulation was 1190 °C and 1170 °C, respectively, which is more accurate than the RC results. The accurate simulation of the fire test was possible due to the implementation of impact spalling effect in the model.

The maximum thermal damage depth of RC and PSC panels from the test and simulation are summarized in Table 2. However,

the comparison results showed remarkable similarity in the simulation results to the test results. The accuracy of the results can be used to conclude that the FE modelling of impact, fire, and impact induced fire simulation models are precise and can be used for more complex analysis of extreme load applied structural member analysis.

5.5. Analytical application of concrete confining and spalling effect

In the simulation of incidental impact loaded concrete structure, it is critical to calibrate the simulation model to match the simulation results to those from model or actual experimental results. Therefore, in this study, two important conditions are

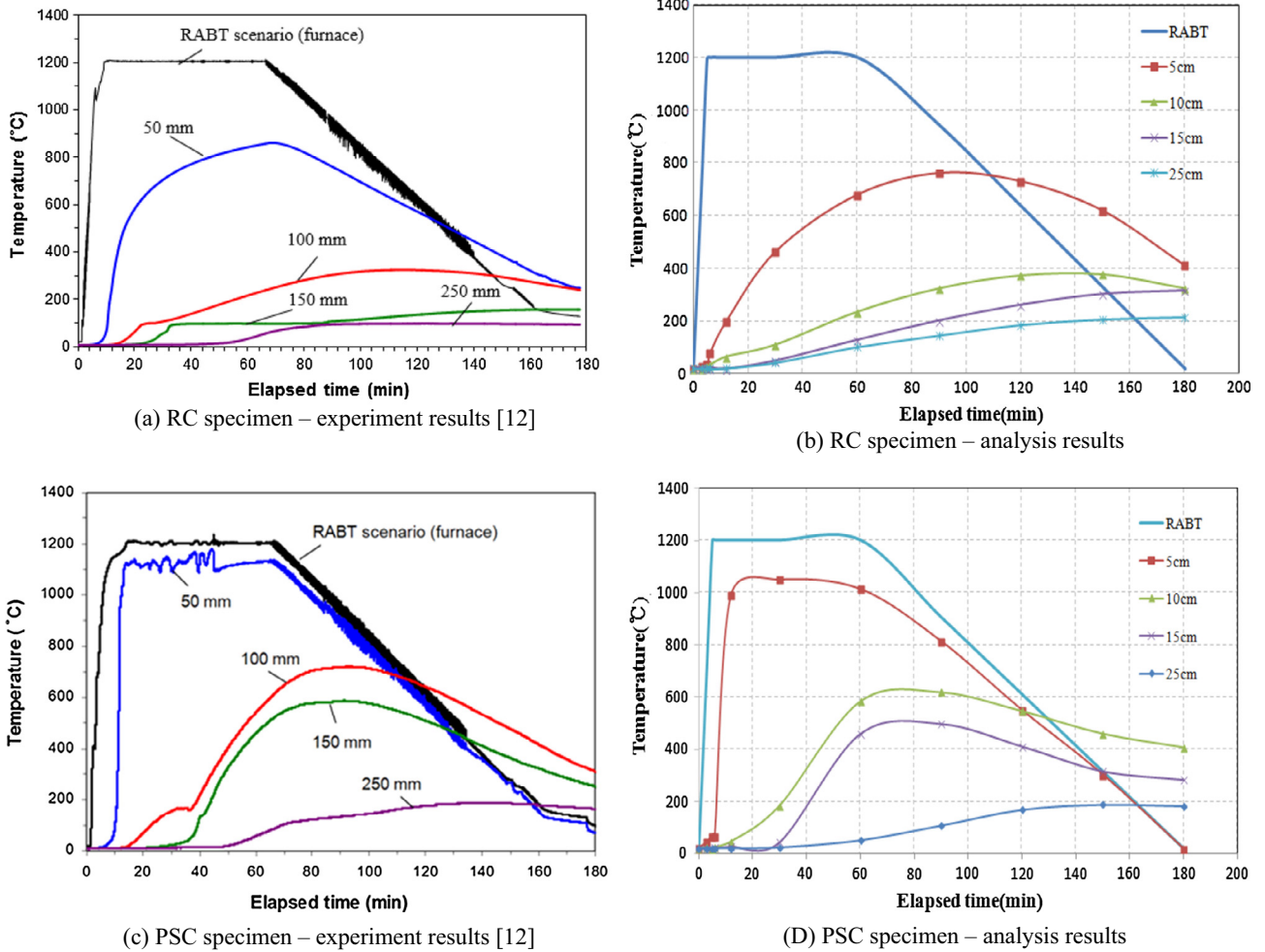


Fig. 23. Temperature variation versus time results from fire only simulation.

Table 1

Experiment and analysis results of RABT fire loading.

	RC specimen		PSC specimen	
	Experiment	Analysis	Experiment	Analysis
Maximum thermal damage depth (mm)	62	70	237	225
Time to reach maximum thermal damage depth (min)	85	90	10	15
Time to expose rebar (min)	17	20	7	10

implemented in the simulation model to calibrate the simulation results. One is the confinement effect of concrete panel induced by prestressing force that enhances the impact resisting performance of the panel. The prestressing confinement effect was implemented by applying initial stress conditions to the prestressing bars to increase the strength of concrete at the inner square region of the panel bounded by PS bars. When the inner confined concrete elements with and without the initial stressing conditions are compared, the results showed that the critical strain exceeding elements ($\epsilon_c > 0.003$) were 16.13% and 11.6%, respectively, in the simulation results. This indicated that the implementation of initial stress condition to PS bars had the intended confinement effect on the inner square section of the panel. Also, the selection of a critical compressive strain of concrete as 0.003 was a proper selection in determining and implementing the spalling effect from impact loading.

When PSC panel is applied with fire loading, severe thermal spalling from the trapping of heated vapor gas within the internal concrete pores from PS confinement effect occurs. Due to the confinement effect of the internal concrete section bounded by PS bars, the thermal spalling volume and severity is much greater in PSC panels than RC panels. In the simulation of fire loaded PSC panels, the initial stress was applied to the PS bars in MIDAS FEA commercial program. However, the simulation results were very different than the test results. In order to calibrate the simulation results to the fire test results, thermal conductivity properties used in the simulation model were varied according to the temperature. Instead of using a constant thermal conductivity value of concrete used in Eurocode 2, thermal conductivity value was increased according to the concrete temperature up to 5 times the Eurocode 2 value to 5.9–12.0 W/m °C. The variation in the thermal conductivity is required due to the confinement effect of prestressed

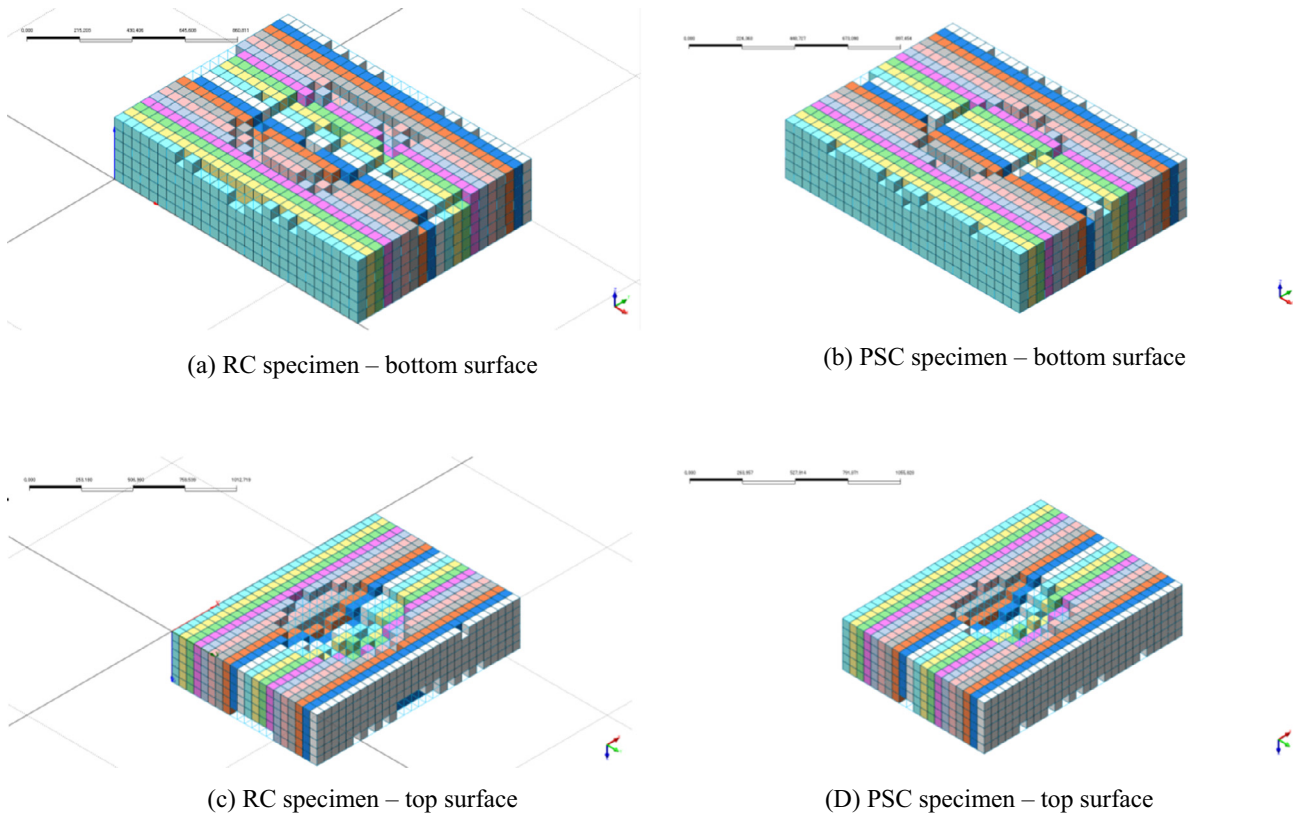


Fig. 24. Finite element modelling of impact damaged specimen for fire simulation in MIDAS FEA.

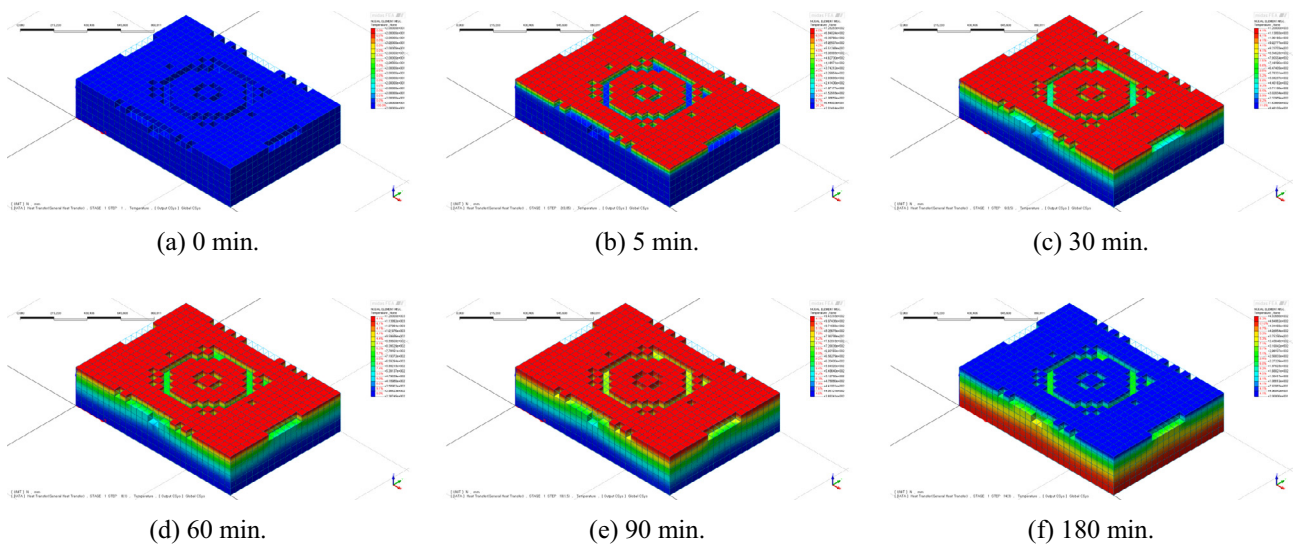


Fig. 25. Temperature distribution of RC specimen from impact induced fire simulation.

concrete where the more dense concrete resulting from prestressing and vapor gaseous effect would increase the thermal conductivity of concrete. The varying of the conductivity value was successful in improving the accuracy of the simulation results to match the test results.

Only fire loaded and impact followed by fire loaded test results were compared. The comparison showed that the temperatures at 5 cm from the heated surface were similar. However, at depths of 10, 15, and 25 cm from the heated surface, the temperatures of impact/fire loaded panels were far lower than those of only fire

loaded panels. The lower temperatures of impact/fire loaded specimen can be attributed to cracks and damages induced by impact loading where they provided paths for internal vapor gased to escape from the specimens. These escape paths can be model in the MIDAS FEA simulation by element elimination technique based on concrete sappling effect as described previously. By eliminating the elements that have compressive strain exceeding a critical strain limit of 0.003, the effect of thermal transfer at the elements with impact cracks and damage can be modeled in the simulation effectively. The external environmental temperature of 20 °C was

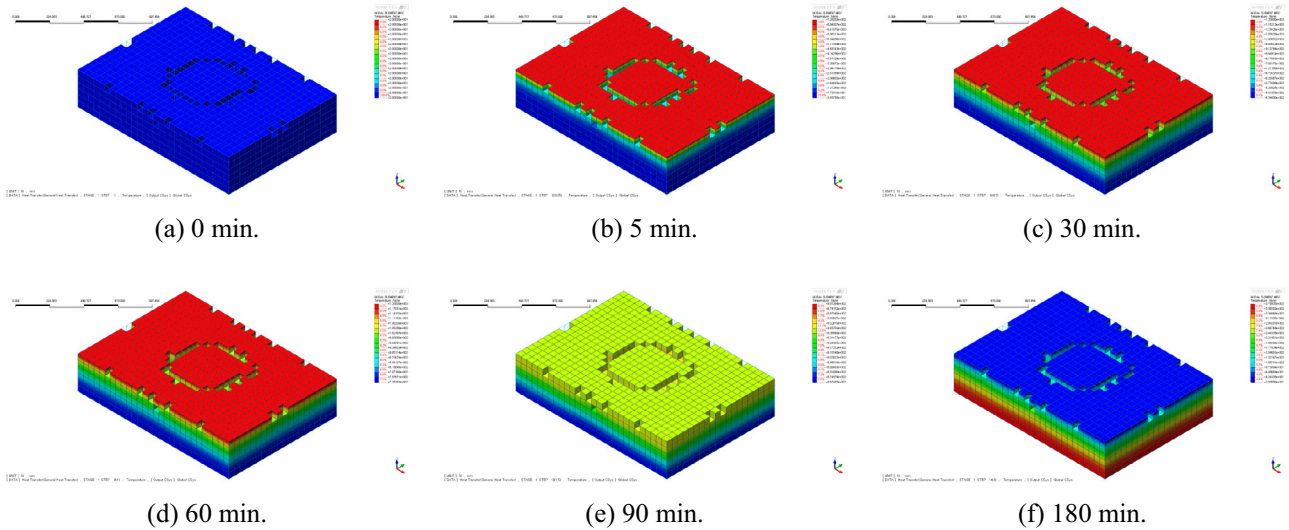


Fig. 26. Temperature distribution of PSC specimen from impact induced fire simulation.

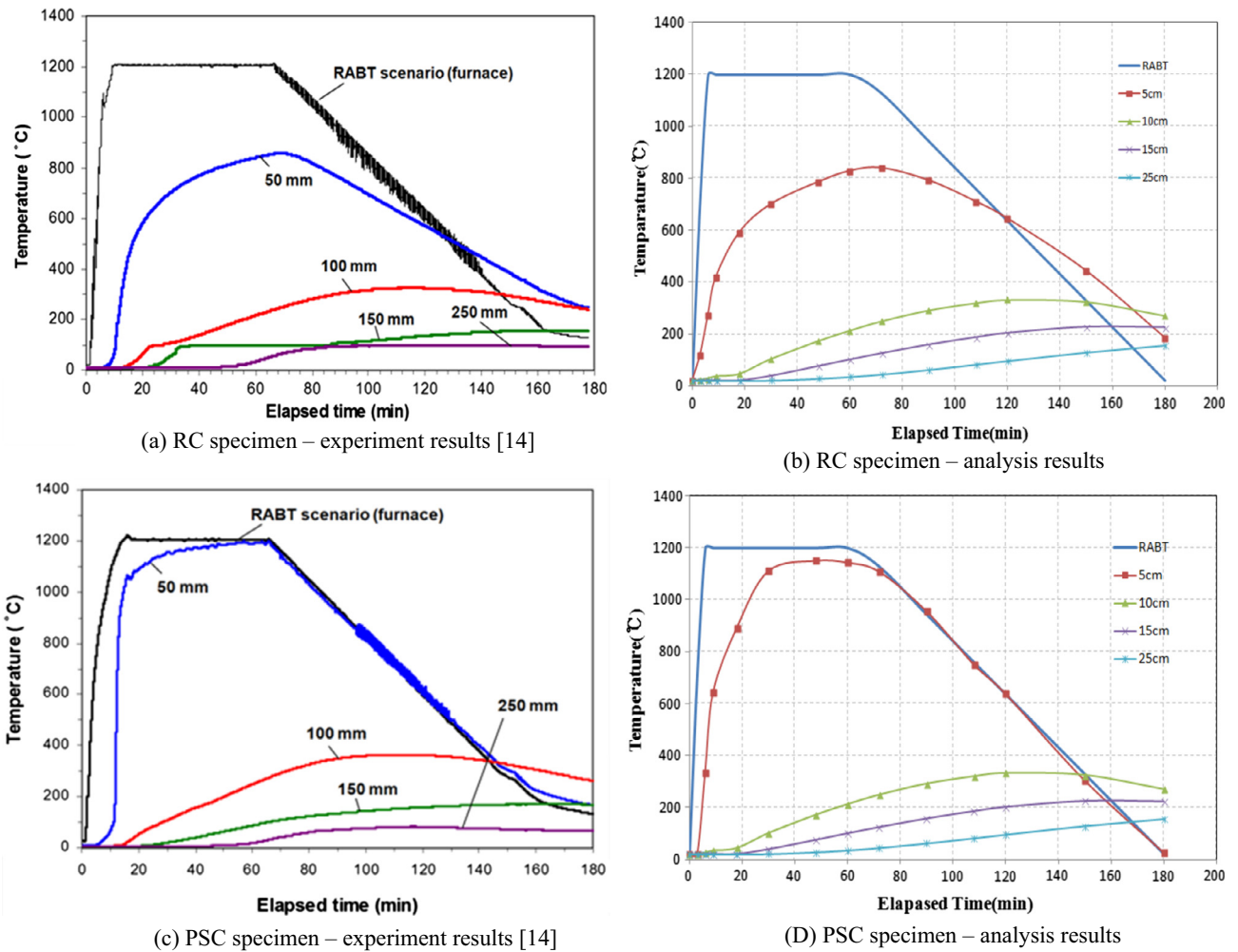


Fig. 27. Temperature versus time results from impact induced fire simulation.

applied to the specimen surfaces that was not fire loaded. Based on the simulation results obtained from the model with the concrete spalling effect, even though a slightly higher temperature at a depth of 25 cm was observed in the simulation results than in

the test results, the temperature results obtained at various specimen depths from the simulation and test are in close agreement as shown in Figs. 23 and 27. Therefore, the thermal conductivity variation and concrete element elimination technique implementations

Table 2
Comparison of fire and impact induced fire simulation results.

Specimen type	Maximum thermal damage depth (mm)			
	Impact induced fire		Fire	
	Experiment	Analysis	Experiment	Analysis
RC specimen	64	70	62	70
PSC specimen	65	80	237	225

contributed effectively in calibrating the simulation results to the test results.

6. Conclusions

The structural performance evaluations of PSC panels from impact induced fire load were analytically carried out. The following conclusions can be drawn from the study.

- (1) Simulation results of single extreme loading event such as impact, blast, and fire, the finite element models were shown to be reliable.
- (2) When simulating the experimental RABT fire scenario test of PSC panel by implicit FEM analysis, application of temperature dependent thermal conductivity coefficient with a maximum value of 3 times ordinary thermal coefficient for concrete are necessary to obtain accurate simulation results.
- (3) When simulating the experimental impact induced fire test of PSC panel by FEM analyses, application of concrete confinement and spalling effect using initial stress condition on PS bars and element elimination technique on concrete elements are necessary to obtain accurate simulation results.
- (4) The simulation results showed accurate impact damage pattern and concrete temperatures similar to those obtained from low velocity impact and RABT fire scenario test, respectively.
- (5) The analysis procedure of PSC panels under impact induced fire loading can be used as numerical simulation tool for real impact accident scenario of full-scale PSC structures.

Acknowledgements

This work was supported by the Nuclear Safety Research Program through the Korea Foundation Of Nuclear Safety (KOFONS), granted financial resource from the Nuclear Safety and Security Commission (NSSC), Republic of Korea (No. 1403010). Also, this work was partially supported by the National Research Foundation of Korea (NRF) grant funded by the Korea government (MSIP) (No. 2016R1A2B3009444).

References

- [1] Yi NH, Kim JHJ, Han TS, Cho YG, Lee JH. Blast-resistant characteristics of ultra high strength concrete and reactive powder concrete. *Constr Build Mater* 2012;28(1):578–84.
- [2] Ha JH, Yi NH, Choi JK, Kim JHJ. Experimental study on hybrid CFRP-PU strengthening effect on RC panels under blast loading. *Compos Struct* 2011;93(1):2070–82.
- [3] Mays GC, Smith PD. Blast effect on buildings: design of buildings to optimize resistance to blast loading. London: Thomas Telford; 1995.
- [4] Jeon SJ, Jin BM, Kim YJ. Assessment of the fire resistance of a nuclear power plant subjected to a large commercial aircraft crash. *Nucl Eng Des* 2012;247:11–22.
- [5] Hou X, Zheng W, Kodur VKR. Response of unbonded prestressed concrete continuous slabs under fire exposure. *Eng Struct* 2013;56:2139–48.
- [6] Christopher DE, Elin J. Reliability analysis of prestressed concrete beams exposed to fire. *Eng Struct* 2010;43:69–77.
- [7] Moon IH, Noh SH, Lee SY, Kim KJ. Structural behavior of PSC reactor containment structure under temperature and pressure loading. *J KSCE* 2007;27(6A):847–58 [in Korean].
- [8] Moss PJ, Dhakal RP, Wang G, Buchanan AH. The fire behaviour of multi-bay, two-way reinforced concrete slabs. *Eng Struct* 2008;30(12):3566–73.
- [9] Won JP, Choi SW, Park CG, Park HK. Temperature distribution of wet-mixed high strength sprayed polymer mortar for fire resistance of tunnel. *J KSCE* 2006;26(4C):283–90 [in Korean].
- [10] Ring T, Zeiml M, Lackner R. Underground concrete frame structures subjected to fire loading: part I: large-scale fire tests. *Eng Struct* 2014;58:175–87.
- [11] Bailey CG, Ellobody E. Fire tests on bonded post-tensioned concrete slabs. *Eng Struct* 2009;31(3):686–96.
- [12] Yi NH, Choi SJ, Lee SW, Kim JHJ. Failure behavior of unbonded bi-directional prestressed concrete panels under RABT fire scenario. *Fire Saf J* 2015;71:123–33.
- [13] Yi NH, Lee SW, Kim JW, Kim JHJ. Impact-resistant capacity and failure behavior of unbonded bi-directional PSC panels. *Int J Impact Eng* 2014;28(1):578–84.
- [14] Yi NH, Lee SW, Choi SJ, Kim JHJ. Performance evaluation of PSC panel from impact-induced fire loading. *MA CR* 2015;67(23):1257–73.
- [15] Nam JW, Kim JHJ, Kim SB, Yi NH, Byun KJ. A study on mesh size dependency of finite element blast structural analysis induced by non-uniform pressure distribution from high explosive blast wave. *KSCE J Civil Eng* 2008;12(4):259–65.
- [16] Agarwal A, Varma AH. Fire induced progressive collapse of steel building structures: the role of interior gravity columns. *Eng Struct* 2014;58:129–40.
- [17] Ali F, Nadjai A, Choi S. Numerical and experimental investigation of the behavior of high strength concrete columns in fire. *Eng Struct* 2010;32(5):1236–43.
- [18] Sugano T, Tsubota H, Kasai Y, Koshika N, Ohnuma H, von Riesenmann WA, et al. Local damage to reinforced concrete structures caused by impact of aircraft engine missiles. Part 1. Test program, method, and results. *Nucl Eng Des* 1993;140:387–405.
- [19] Murray YD. User manual for LS-DYNA concrete material Model 159. Federal Highway Administration; 2007.
- [20] Murray YD. Evaluation of LS-DYNA concrete material Model 159. Federal Highway Administration; 2007.
- [21] Malvar LJ, Crawford JE, Wesevich JW, Simons D. A plasticity concrete material model for DYNA3D. *Int J Impact Eng* 1997;19(9–10):847–73.
- [22] Nam JW, Kim HJ, Kim SB, Kim JHJ, Byun KJ. Analytical study of finite element models for FRP retrofitted concrete structure under blast loads. *Int J Damage Mech* 2009;18(5):461–90.
- [23] Jiang H, Wang X, HE S. Numerical simulation of impact tests on reinforced concrete beams. *Mater Des* 2012;39:111–20.
- [24] Eurocode 2. Design of concrete structure part 1, 2 general rules-structural fire design, DO ENV; 1992.
- [25] Hallquist JO, Waincott B, Schweizerhof K. Improved simulation of thin-sheet metal forming using LS-DYNA 3D on parallel computers. *J Int Process Tech* 1995;50(1):144–57.